LAWRENCE
LIVERMORE
NATIONAL
LABORATORY

UCRL-PROC-224033

First X-ray Fluorescence MicroCT Results from Micrometeorites at SSRL

K. Ignatyev, K. Huwig, R. Harvey, H.A. Ishii, J.P. Bradley, K. Luening, S. Brennan, P. Pianetta

August 23, 2006

9th International Conference on Synchrotron Radiation Instrumentation
Daegu, North Korea
May 28, 2006 through June 2, 2006

First X-ray Fluorescence MicroCT Results from Micrometeorites at SSRL

Konstantin Ignatyev[1], Kathy Huwig[2], Ralph Harvey[2], Hope Ishii[3], John Bradley[3], Katharina Luening[1], Sean Brennan[1], Piero Pianetta[1]

[1] *Stanford Synchrotron Radiation Laboratory, 2575 Sand Hill Rd, Menlo Park, CA 94025, USA*
[2] *Case Western Reserve University, Cleveland, OH 44106, USA*
[3] *Lawrence Livermore National Laboratory, 7000 East Avenue, Livermore, CA 94550, USA*

Abstract. X-ray fluorescence microCT (computed tomography) is a novel technique that allows non-destructive determination of the 3D distribution of chemical elements inside a sample. This is especially important in samples for which sectioning is undesirable either due to the risk of contamination or the requirement for further analysis by different characterization techniques. Developments made by third generation synchrotron facilities and laboratory X-ray focusing systems have made these kinds of measurements more attractive by significantly reducing scan times and beam size. First results from the x-ray fluorescence microCT experiments performed at SSRL beamline 6-2 are reported here. Beamline 6-2 is a 54 pole wiggler that uses a two mirror optical system for focusing the x-rays onto a virtual source slit which is then reimaged with a set of KB mirrors to a (2 x 4) μm^2 beam spot. An energy dispersive fluorescence detector is located in plane at 90 degrees to the incident beam to reduce the scattering contribution. A PIN diode located behind the sample simultaneously measures the x-ray attenuation in the sample. Several porous micrometeorite samples were measured and the reconstructed element density distribution including self-absorption correction is presented. Ultimately, this system will be used to analyze particles from the coma of comet Wild-2 and fresh interstellar dust particles both of which were collected during the NASA Stardust mission.

Keywords: tomography, microprobe.
PACS: 87.59.Fm

INTRODUCTION

Computed tomography (CT) allows reconstruction of 3D information about the inner structure of an object without the need for sample preparation such as sectioning. X-ray absorption CT is well known and is widely used in medicine (CAT scan) as a diagnostic tool. Initially CT measurements were performed on large samples but as technique and technology improved, smaller samples also became a focus of CT studies. MicroCT is a variant of CT that deals with samples which are smaller in size than 1 mm. Recently, a new mode of CT has emerged that employs the detected fluorescence signal of the sample – X-ray fluorescence CT – allowing for the measurement of trace elements. This technique only became feasible with third generation synchrotron sources producing high brightness x-ray beams and the availability of focusing optics [1, 2].

In this work X-ray microCT measurements were conducted on two micrometeorites collected in the Antarctic field. Typically, collected micrometeorites range widely in their internal morphology. MicroCT measurements were used to compare their internal structure non-destructively.

EXPERIMENTAL

The back hutch of the SSRL Wiggler beam line 6-2 was used to collect the data on two Antarctic micrometeorites (100 μm diameter). For the purpose of their easy identification they were named “Mike” and “Olga”. Their external morphology and appearance is quite different as can be seen on the optical micrographs in

Fig. 1. “Olga” has rough external morphology with a lot of bubble-like structures on the surface which suggests a highly vesicular inner structure. Mike on the other hand has a smooth ovoid shape. The meteorites were mounted on top of a silica capillary tube with good mechanical stability. First, X-ray fluorescence spectra were collected at several positions on the micrometeorites with collection times of 200 sec for the purpose of determining their average composition. The incident photon energy was 11 keV. As shown in Fig. 2, an energy-dispersive detector was placed in-plane at 90 degree angle to the incident beam to reduce the scatter contribution. The sample can be rotated and translated in the X-ray beam by a high precision rotation stage mounted on top of a high precision x-y-z translation stage. In addition, the sample can be centered relative to the axis of rotation by a miniature x-y-z stage mounted directly on the high precision rotation stage. The horizontal beam sizes used varied from 2 to 4 μm and vertical beam sizes varied from 3 to 4 μm. The scanning geometry is identical to the one used in 1st generation CT scanners which are based on a pencil beam: the sample is translated first in the direction perpendicular to the beam, rotated a predetermined angle and then the sequence is repeated. The translation step size for all scans was equal to the horizontal beam size. We simultaneously collected the X-ray transmission signal with the photodiode located directly behind the sample. One scan took from 5 to 8 hours depending on the translation step size and number of projections.

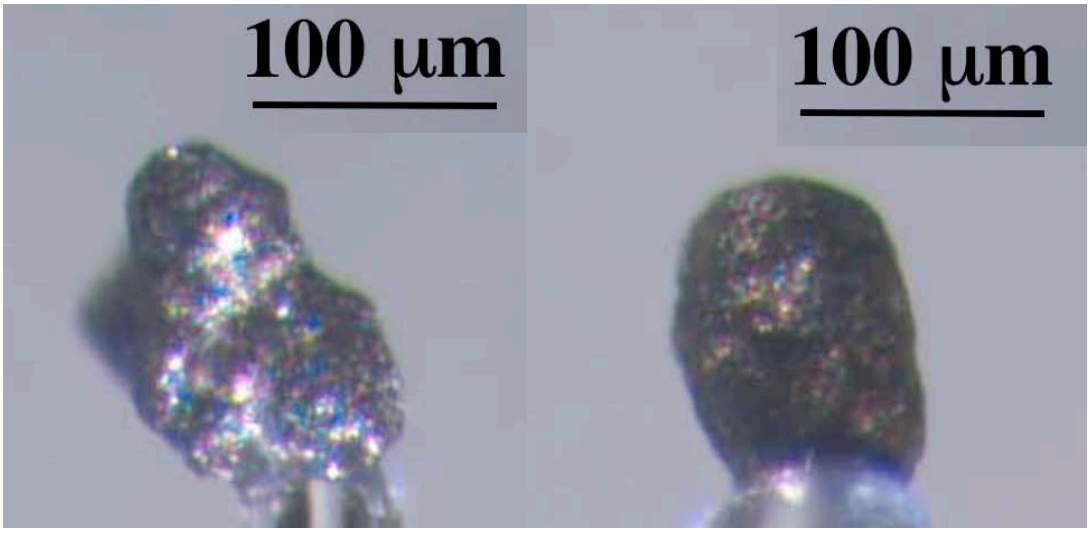

FIGURE 1. Optical micrographs of “Olga” (on the left) and “Mike” (on the right)

RESULTS AND DISCUSSION

For “Mike”, fluorescence CT reconstructions were done using the algebraic reconstruction approach as described in [3], employing the Kaczmarz iterative method for solving the system of linear equations. While absorption CT reconstruction is rather straightforward, fluorescence CT is challenging, especially for samples with high X-ray attenuation. X-ray self-absorption in the sample has to be taken into account when measuring highly attenuating samples. The following expression can be used to describe the fluorescence signal excited by the incident X-ray beam in the sample (neglecting second-order effects such as secondary fluorescence):

$$p_{ab}^{i} = I_0 \xi_{fluor} \varpi^{i} \int_a^b \mu_0^{i}(x) \exp\left[-\int_a^x \mu_0(x')dx'\right] \exp\left[-\int_{L(x)} \mu_{fluor}^{i}(x,y)dy\right] dx$$

where superscript i refers to the element of interest, p_{ab} is the measured fluorescence signal for a specific sample position and orientation, I_0 is the intensity of the incident radiation, ξ_{fluor} is the fluorescence detector efficiency, ϖ is

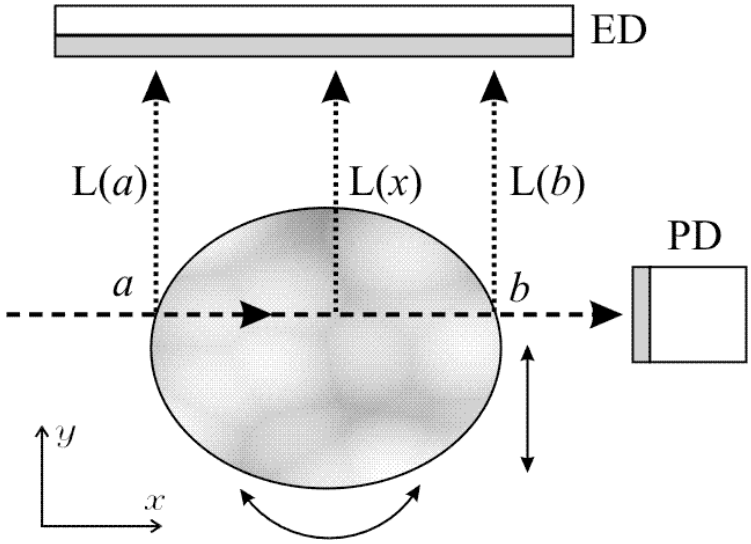

FIGURE 2. Schematic of the X-ray beam passing through a sample with fluorescent radiation measured by the energy dispersive detector ED and transmitted radiation measured by the photodiode PD. L(x) is the line connecting source of the fluorescence radiation at position *x* with the energy-dispersive detector. Incident beam enters the sample at position *x=a* and exits the sample at *x=b*. Sample is translated in the horizontal plane in the direction perpendicular to the beam and rotated about the vertical axis.

the fluorescence yield, μ^i_0 is the linear attenuation coefficient of the *i*th element at the X-ray incident beam energy, μ_0 is the linear attenuation coefficient of the sample at the incident energy and μ^i_{fluor} is the linear attenuation coefficient of the sample for the *i*th element fluorescence. Applying this expression for each beam trace (for each sample translation and rotation) forms a set of equations that can be solved iteratively.

Absorption of the incident radiation for each point and orientation of the sample can be calculated from the absorption map reconstructed from the X-ray transmission signal. The second part of the self-absorption correction dealing with the absorption of the elemental fluorescence signal on its way to the detector is considerably more challenging. One approach exists that allows calculating the absorption of the fluorescence signal without making assumptions about the sample if all major absorbers in the sample fluoresce [4]. Another way to do it is to measure the sample attenuation for all incident beam energies equal to the energies of the fluorescent lines of the elements that are present in the sample, however this is time consuming. For this preliminary study the following assumption was made to facilitate the application of the corrections for self-absorption of fluorescent radiation in the micrometeorites: since Fe is the major constituent in these types of samples, absorption by all the other elements in the sample was assumed to be negligible compared to iron. Thus, the iron distribution was taken to follow the reconstructed attenuation map and could be used to calculate the self-absorption for the fluorescence signal from the elements of interest for all points and orientations of the sample. This approach will introduce errors if the iron distribution is not uniform with respect to the absorption in the sample, however, in our case the reconstructed map of the iron fluorescence showed little deviation from the absorption map in the regions close to the surface (where the absorption correction is small) as well as in the regions closer to the center of the sample.

Figures 3a and 3b show the absorption microtomography reconstructions of two micrometeorites. They were done using filtered backprojection with a Shepp-Logan filter [3]. This dataset was collected with a (2 x 2) μm^2 beam size and the reconstructed pixel size was 2 μm. These images clearly show that although the external morphology is quite different for the two samples, both of them contain large voids and a number of smaller vesicles.

Figures 3c and d show the output of the iterative algebraic reconstruction used on "Mike" (at a different location compared to what is shown on Fig. 3b). Fig. 3c shows the density map of the sample that was used for the self absorption correction. It was used directly for the 11 keV incident beam attenuation correction. In order to correct for the attenuation of the fluorescent radiation it was normalized to the change in the linear attenuation coefficient of iron at the fluorescent energies of Fe Kα and Ni Kα. The reconstructed Ni density map (Fig. 3d) shows a strong Ni contribution in the center of the micrometeorite. This high density grain can also be seen on the absorption map at the same location as the Ni-rich structure.

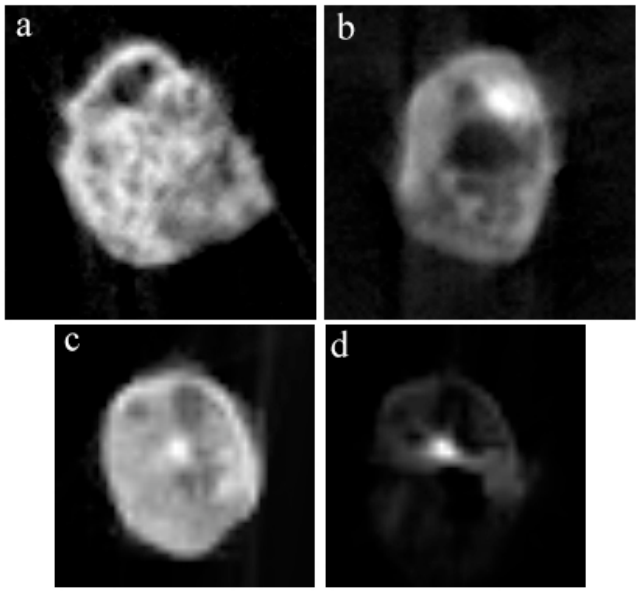

FIGURE 3. Top row - comparison of the density maps of (a) "Olga" and (b) "Mike" obtained with absorption CT reconstruction of a single slice in transmission (beam size 2 μm, angular step size 2° in 180°, number of translation steps 80, integration time 1 s per point, total measurement time 4 hours, resolution 2 μm). Brighter pixels correspond to higher x-ray attenuation by the sample and darker pixels to lower. Bottom row – algebraic reconstruction images of "Mike": (c) absorption and (d) Ni distribution maps (beam size 4 μm, angular step size 4° over 180°, total number of translation steps 50, integration time 4 seconds, total measurement time 3 hours, resolution 4_m). Fluorescent signals for Fe and Ni were ~$3x10^4$ and $1x10^4$ Hz at the peak, respectively. For (c) brighter pixels correspond to higher X-ray attenuation and for (d) brighter pixels correspond to higher elemental concentrations. Field of view of each image is 130 μm.

CONCLUSION

Absorption microCT was used to reconstruct the density cross-section of two micrometeorite samples and it showed that despite differences in external morphology, both of the meteorites had regions of similar internal morphology. Fluorescence microCT was used to determine the distribution of Ni in the cross-section of one of the meteorites. To improve the accuracy of this reconstruction technique, further work will include a modified iterative absorption correction that takes the absorption by all the higher concentration elements in the sample into account.

ACKNOWLEDGMENTS

This research was carried out at the Stanford Synchrotron Radiation Laboratory, a national user facility operated by Stanford University on behalf of the U.S. Department of Energy, Office of Basic Energy Sciences. This research was partially funded by the NASA SRLIDA Program grant number SRL03-0010-0010.

REFERENCES

1. A. Simionovici, B. Golosio, M. Chukalina, A. Somogyi, L. Lemelle, *Developments in X-ray Tomography IV*, SPIE Proceedings, **5535**, 232-242 (2004).
2. D. H. McNear, E. Peltier, J. Everhart, R.L. Chaney, S. Sutton, M. Newville, M. Rivers and D.L.Sparks, *Environ. Sci. Technol*. **39**, 2210-2218 (2005).
3. A. C. Kak and M. Slaney, *Principles of Computerized Tomographic Imaging*, IEEE Press, 1988.
4. M. Chukalina, A. Simionovici, A. Snigirev and T. Jeffries, *X-ray Spectrom.* **85**, 448-450 (2002).
5. IDL absorption CT reconstruction software by Mark Rivers (http://cars9.uchicago.edu/software).

This work was performed under the auspices of the U.S. Department of Energy, NNSA by the Lawrence Livermore National Laboratory under contract No. W-7405-Eng-48.